REACTIVE SINTERING OF MnZn FERRITES[†]

Tomaž Kosmač[a] and Mihael Drofenik[b]
[a]*Jožef Stefan Institute, Jamova 39, SI-1000 Ljubljana, Slovenia*
[b]*Faculty for Chemistry and Chemical Engineering, University of Maribor,*
Smetanova 17, SI-2000 Maribor, Slovenia

[†]This paper is dedicated to the late Professor Dr. Drago Kolar

Received 29-01-2001

Abstract

Reaction-formed MnZn ferrite was prepared and the decrease in shrinkage after sintering due to the volume expansion accompanying iron oxidation was studied.

Green compacts consisting of the milled raw oxides Fe_2O_3, Mn_3O_4, ZnO and metallic iron powder were sintered at 1350 °C in air. During the first hold at 800 °C, Fe was oxidized to α-Fe_2O_3 and Zn ferrite was formed. Above 1300 °C the reaction bonding was completed and MnZn ferrite, exhibiting a relatively low shrinkage, was formed. The chemical reactions involved during reaction bonding were associated with a volume expansion and porosity formation, compensating for the shrinkage on sintering. Intensive milling decreases the porosity after sintering but induces the oxidation of iron, and partially removes the shrinkage compensation caused by the presence of metallic iron.

Introduction

The magnetic properties of MnZn ferrites depend strongly on the processing parameters and the technology used during the production of ferrite ceramics.[1] The ceramic route is usually chosen to prepare ferrite cores as this procedure is relatively simple to perform and convenient for large-scale production. In some cases so-called "green" technology can also be applied for the production of relatively large and less complex products. Recently, the reaction sintering which accompanies the densification of "green" compacts was studied.[2,3] This route simplifies the ferrite processing since the calcination during ferrite production is omitted. In general, this technology is avoided because of the difficulties associated with low powder compressibility and the relatively large shrinkage after sintering. The inhomogeneities induced during compacting with pressure result in variable shrinkage during sintering, deformation of the samples and crack formation. The application of rate-controlled sintering[4] can improve the situation; however, extensive sample shrinkage during densification still cannot be eliminated. In order to decrease the relatively large shrinkage occurring, the reaction forming[5,6] of MnZn ferrite can involve the replacement of some of the Fe_2O_3 by iron in the original raw material.

In this technique, homogenised and milled Fe_2O_3/Fe, MnO and ZnO compacts are heated in air so that iron metal is oxidised to hematite, which then reacts with the rest of the oxides forming MnZn ferrite. The oxidation of iron is associated with a volume expansion, which can accelerate the reaction and compensate for the shrinkage during densification. A general equation which can predict the total dimensional change (S) after the reaction forming during sintering is given by:

$$S = \left(\frac{1 + w \cdot V \cdot \rho_O / \rho}{1 + 0.28 \cdot f \cdot V} \right)^{1/3} - 1 \qquad (1)$$

where w is the volume expansion accompanying the respective oxidation, i.e. w = 1.13, V is the volume fraction of the metal added to the original powder mixture; f is the Fe fraction oxidised during milling; and ρ_o and ρ are the "green" and final densities, respectively.

The aim of this work was to study the reaction-sintering process and the microstructural development of reaction-formed MnZn ferrite cores.

Experimental

MnZn ferrite with a final composition $Mn_{0.6}Zn_{0.4}Fe_{2.0}O_4$ was prepared from starting oxides: Fe_2O_3 (99.7 %; SH/Mitsubishi), Mn_3O_4 (99.5 %; Fermac), ZnO (99.8 %; Zinkweiss/Fermac A) and metallic iron (99.8 %; Ventron). Powder materials with different amounts of metallic iron powder (see Table I) were milled in a ball mill and in an attritor mill with alcohol for various periods. After drying, the powders were passed through a 300 μm sieve. Compacts of dimensions O = 10 mm, h = 10 mm were pressed from the sieved power at 200 MP. The exact dimensions were measured before and after the heat treatment. "Green" densities were determined from the sample weights and dimensions.

The homogenized and milled powders were characterized by TGA, DTA and SEM. The average grain size and its distribution was measured using a Cilas/Alcatel-granulometer. The porosity of the green compacts and sintered samples was determined using a Carlo Erba Porosimeter. The microstructure of polished and etched sintered samples was inspected by SEM and optical microscopy. Dilatometric experiments were carried out on a push-rod dilatometer with a temperature limit of 1400 °C. The samples were sintered in air at 1350 °C for 6 hours, in some cases a nitrogen atmosphere was also used during the sintering. The samples were cooled in a controlled atmosphere with the amount oxygen according to $\log PO_2 = -14{,}406/T + 9.64$, where PO_2 is in % and T is in K. O_2/N_2 mixtures were supplied by a partial oxygen pressure unit, while heating and cooling were controlled with a digital temperature controller.

Table I: The amount of iron oxide added to the starting powder mixture and the amount of iron oxide formed via iron oxidation during reaction forming

Sample code	$Fe_2O_3^{\#}$	$Fe_2O_3^{*}$
O	100 %	0 %
A	79 %	21 %
B	50 %	50 %
C	30 %	70 %
D	0 %	100 %

[#] The amount of Fe_2O_3 added to the raw mixture
[*] The amount of Fe_2O_3 formed via Fe oxidation

Results and Discussion

In order to homogenise the starting powder mixtures and to reduce the particle size, planetary and attritor milling was used. The particle size distribution of the milled powder mixtures vs. milling time for various batch compositions and milling procedures is shown in Figure 1. As a reference, the milling ability of a pure oxide powder mixture without any metallic Fe was examined first (Figure 1a). In spite of a broad particle size distribution of the starting powder blend (due to the different sizes of individual oxide powders) milling in a planetary mill results in a rather uniform, i.e. normal particle size distribution, after 9 hours of milling.

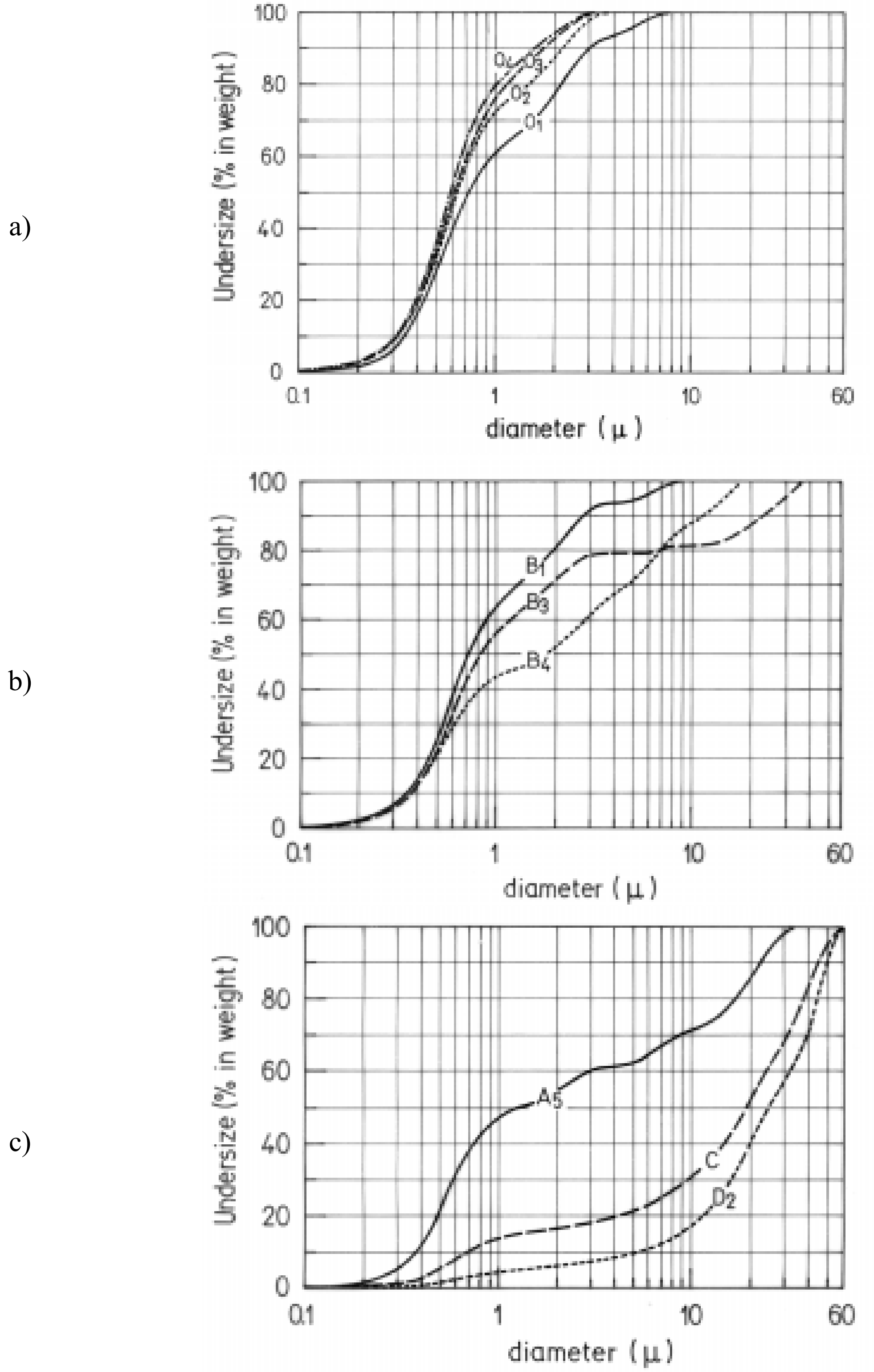

Fig. 1: Cumulative particle size distribution of milled powder mixtures: a) powder 0 (pure oxides) milled 1, 3, 9 and 27 hours in a planetary mill, b) powder B milled 1 and 3 hours in a planetary mill and 7 hours in an attritor mill, c) powders A5, D2 and C milled in an attritor mill. (See Table II for sample codes)

Any further increase in the milling time does not bring about any significant improvement, nor does it result in a re-agglomeration of particles**.** The presence of metal iron particles in the staring powder blend changes the comminuition behaviour resulting in a bimodal particle size distribution. The percentage of the coarse fraction increases with increasing milling time and milling efficiency (Figure 1b), as well as with increasing Fe/Fe_2O_3 ratio in the starting powder blend (Figure 1c). The morphology of powders A and C after attritor milling is represented in Figures 2a and 2b, respectively. Based on the shape complexity, which resembles mechanically alloyed metal powders, it is assumed that most large agglomerates consisting of sub-micron size particles are formed by plastic deformation and welding of metallic particles.

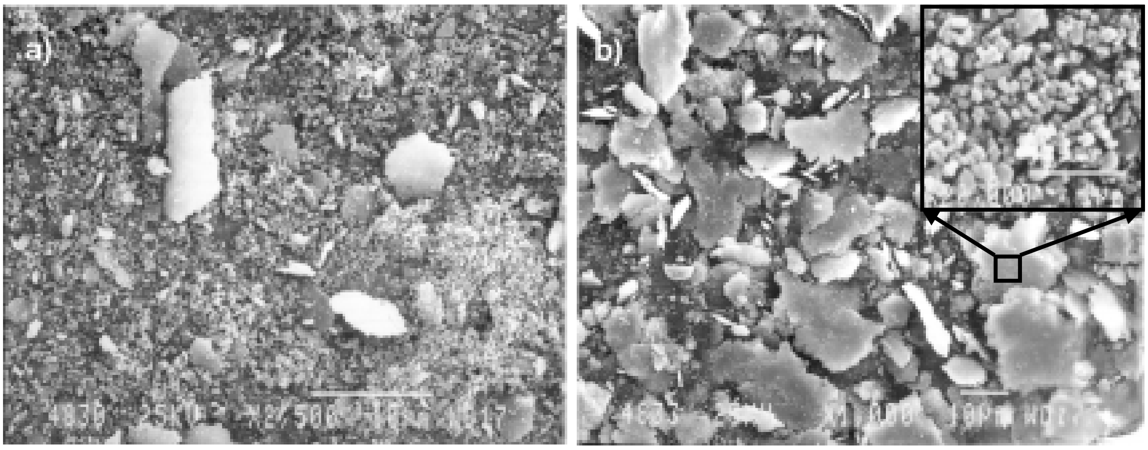

Fig. 2: SEM micrograph of powders A (a) and C (b) after attritor milling for 7 hours

According to the results of electron diffraction (SAD) and EDXS analysis with a TEM (Figure 3), there are two types of sub-micron-sized particles forming the fine structure of the milled metal-oxide powder mixture: monolithic fragments of the constituent oxides, and metallic particles with a diffraction pattern characteristic of α Fe. EDXS analysis of these metallic particles revealed the presence of a small amount of oxygen indicating the partial oxidation of iron during milling. Based on these results it can be concluded that, under the milling conditions used in this work, no extensive mechanochemical reaction has taken place, except for partial oxidation and/or hydration of iron particles. In an earlier study[7] we showed that $ZnFe_2O_4$ can readily be formed from Fe_2O_3 and ZnO powders, by dry milling in a high-energy shaker mill; in a similar way nonequilibrium FeO and (Fe,Zn)O can be formed from Fe_2O_3 and metallic Fe and Zn powder, respectively. Since none of these phases could be detected in our powders, it can be concluded that the milling efficiency of the devices used in this work is not sufficiently high to initiate any of the above mechanochemical reactions.

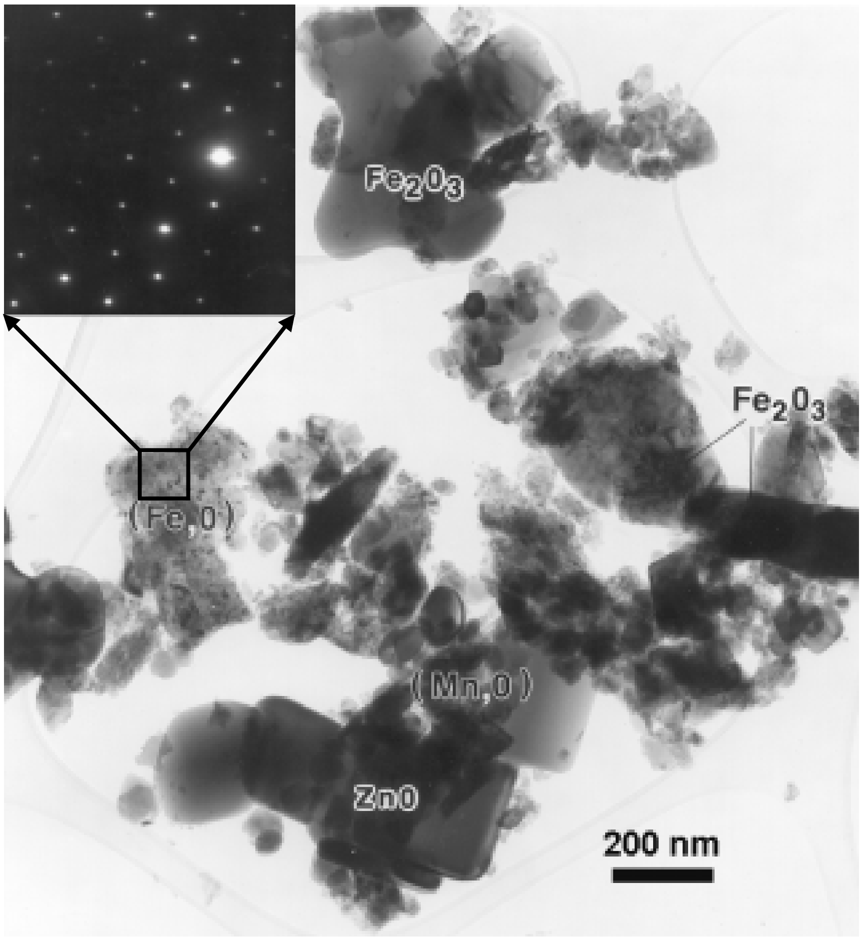

Fig. 3: TEM image of powder B wet milled in an attritor for 7 hours

In order to follow the oxidation behaviour of milled powders during heating in air, TGA was performed and the results are presented in Figure 4. The mass gain of the powders milled in a planetary mill corresponds well to the predicted value, which was calculated by assuming the complete oxidation of the iron in the starting powder blend and the $Mn^{2+}\rightarrow Mn^{3+}$ conversion. For the attritor-milled powders, in contrast, the measured values are lower than predicted, confirming that during milling these powders were partially oxidised and/or hydrated. Also worth mentioning is that the higher the Fe/Fe_2O_3 ratio in the starting powder blend, the lower the temperature at which the oxidation starts. The complexity of partially oxidised and/or hydrated particles, which is reflected in step-wise mass gain of the attritor–milled powders C and D, was not studied in details. Nevertheless, at about 700°C the oxidation of all samples is completed, regardless on the starting Fe/Fe_2O_3 ratio in the powder blend and the milling procedure used.

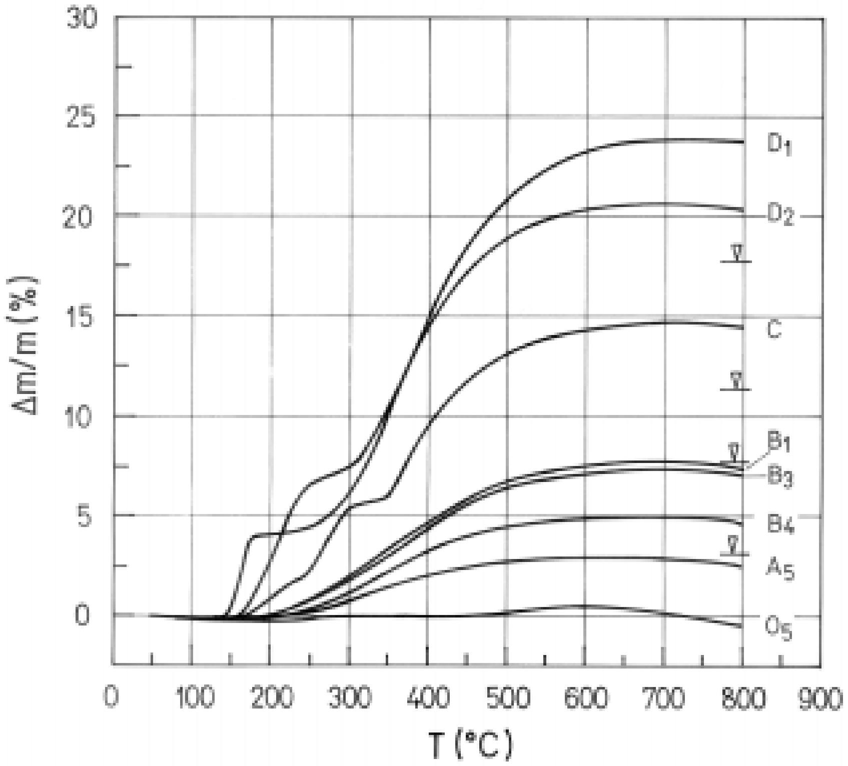

Fig. 4: Mass gain of the starting mixtures 0, A, B and D milled in a planetary ball mill and in an attritor mill for various times as indicated in Table II.

Dilatometric curves of the green compacts obtained from the powder blend B are shown in Figure 5. They illustrate the effect of powder milling on the dimensional changes, which occur with reaction forming of MnZn ferrites.

Sample B1, which was milled for 1 hour in a planetary mill, exhibits a noticeable expansion in the temperature range between 500 and 800°C. In this temperature interval the oxidation of iron is completed (cf. Figure 4) and Zn ferrite is formed. This is clear from the XRD pattern obtained from the B1 powder compact after heat treatment at 600°C. For both reactions the molar volume of the reaction product is larger than that of the solid reactants involved. Furthermore, the reaction product is formed on the surface of relatively large reactant particles, separating them until they disappear. Under these conditions, chemical reactions are usually associated with an observable expansion. Therefore, with powder blends C and D, in which the iron content is high and the coarse agglomerate fraction is prevailing, a substantial expansion associated with the oxidation of iron can be expected too. If, however, the particle size distribution of the reactants is broad enough to allow filling of the interstitial voids between the larger particles with the smaller ones, the linear expansion of the powder compact due to a chemical reaction will be less pronounced or even negligible. This seems to be the case with powders B3 and B4. Also with reference to Figure 5, milling of the starting powder blend has a strong impact on the subsequent densification of the powder compacts. The attritor–milled sample B4 starts sintering at a lower temperature than powders B1 and B3, which were less intensively milled, and exhibits higher shrinkage upon densification. Improved sintering ability as a result of intensive milling is a commonly reported observation and relates to a reduced diffusion path between powder particles, better homogeneity and an increased specific surface area of the powder.

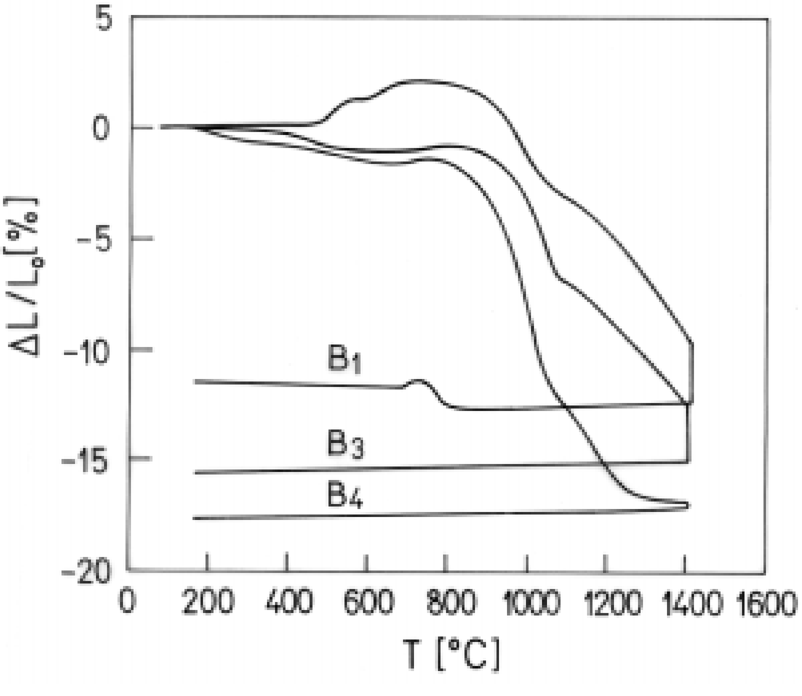

Fig. 5: Dimensional changes of samples B1, B3, wet milled in a planetary mill for 1 and 9 hours, respectively, and B4, milled 7 hours in an attritor mill.

The sintering of green samples was performed with a temperature profile characteristic of MnZn ferrite (see Experimental). The effects of powder composition and milling conditions on sintering shrinkage and the resultant fractional density of sintered MnZn ferrites are summarised in Table II.

Table II: Milling time, specific surface area, green and sintered density, shrinkage and the % of theoretical density (T.D.) for samples sintered at 1350 °C for 16h.

Sample code	Milling time (hours)	Specific surface area (m^2/g)	Green density (g/cm^3)	Sintered density (g/cm^3)	Shrinkage (%)	T.D. (%)
O1	1	5.8	2.80	4.60	16.1	90.6
O2	3	6.2	2.90	4.75	16.2	93.2
O3	9	8.1	2.88	4.80	16.6	94.6
O4	27	10.6	2.87	4.83	16.7	94.7
O5#	7	15.8	2.90	4.77	17.4	93.6
A1	1	6.3	2.91	4.51	14.5	88.3
A2	3	6.4	2.94	4.63	15.0	90.6
A3	9	6.6	2.93	4.76	15.5	92.7
A4	27	8.8	2.91	4.88	16.5	95.7
A5#	7	14.8	2.74	4.79	18.2	93.8
B1	1	5.5	3.10	4.35	9.8	85.3
B2	3	5.7	3.10	4.50	11.0	88.3
B3	9	6.3	3.10	4.53	11.7	88.8
B4#	7	10.3	2.92	4.84	16.0	94.8
C#	4	7.8	3.17	4.04	4.0	79.3
D1#	4	7.1	3.28	3.58	-6.2	70.2
D2	8	7.5	3.07	3.66	-0.5	74.5

#attritor milling

Samples exhibit a relatively large percentage of porosity, which increases with the amount of iron added to the original oxide mixture and decreases with the time of milling (Table II). In Figs. 6 and 7 typical microstructures of samples 0 (milled in a ball mill) and B (milled in an attritor mill) are shown.

From the microstructures of samples prepared from powders milled for various times it can be seen that the porosity of sintered samples decreases with time. Thus, a larger initial specific surface and a higher homogeneity promote the densification of ferrite samples. In green samples without the addition of iron the decrease in the porosity with milling time is remarkable; see Figs. 6a, 6b. When the milling of the starting powders containing iron is prolonged, the porosity of the sintered compacts decreases as well; however, to a somewhat smaller extent. Particularly when the amount of iron is higher a prolonged time of planetary milling is ineffective; see the microstructure in Figs. 7a, 7b, and Table II. On the other hand, when attritor milling is used, which increases the specific surface of the starting powder, the porosity again starts to decrease on sintering, see Table II. In this case abnormal grain growth is observed, the pores become smaller, but are trapped in larger grains, Fig. 7c.

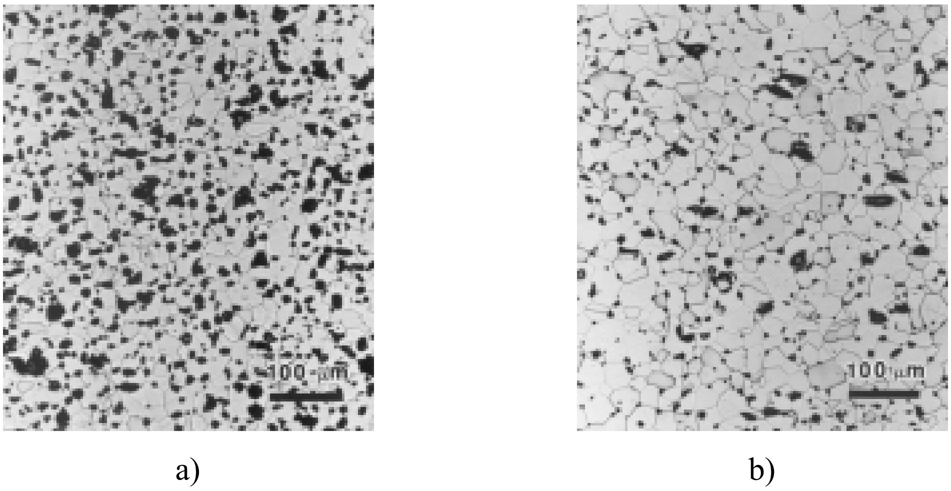

Fig. 6: Microstructure of samples O1 (a) and O3 (b) milled in a planetary mill for 1 and 9 hours, respectively.

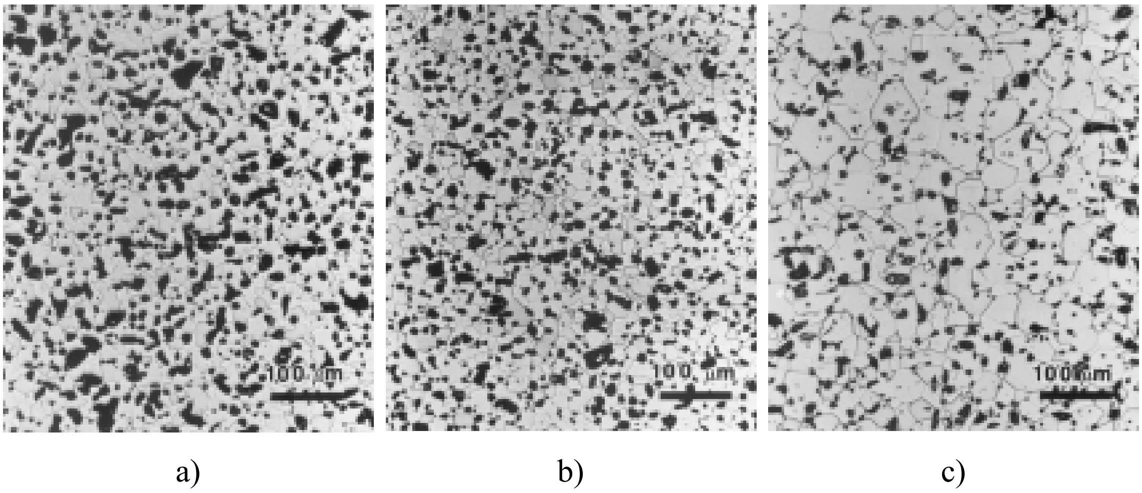

Fig. 7: Microstructure of samples B2 (a) and B3 (b) milled in a planetary mill for 3 and 9 hours, respectively, and of sample B4 (c) milled in an attritor mill for 7 hours.

When we try to compensate for the shrinkage during sintering by using metal iron powders, the extent and the number of chemical reactions during the heat treatment is important and must be considered.

Three main reactions govern the formation of ferrite cores: i) the oxidation of iron to haematite between 200 – 600 °C, Fig. 3; ii) the formation of Zn ferrite between 600-700 °C, and iii) the formation of mixed MnZn ferrite above 900 °C. Thus, it is quite reasonable to expect that the porosity induced during reaction forming, which is a result of the reaction sintering in a metal-iron containing MnZn-ferrite composite, must be relatively large and should be carefully considered.

The porosity in green MnZn-ferrite composites prepared from calcined ferrite powders is induced during ferrite-powder compaction. This initial porosity then gradually decreases during sintering, depending on the relationship between coarsening and densification. However, in parallel with the chemical reactions accompanying the ferrite formation and sintering, an additional porosity is formed. Besides, the inhomogeneous densification caused by a broad particle size distribution, as well as Kirhendall porosity induced by unequal mutual diffusion of the reactants, can increase the final pore size. Large pores, when formed, are extremely unfavourable, since their elimination during sintering is practically impossible.[8,9]

We observed during our study that the most effective way to improve the microstructure and to decrease the porosity is by using intensive milling. However, intensive milling also induces the partial oxidation of iron due to mechanochemically induced reactions.

Based on the experimental work performed during this study, Table I and II, an interrelation between the density and the shrinkage of sintered composite samples O, A, B, C and D containing various amounts of metal iron can be matched in a graph as shown in Fig. 8.

As was expected, and then experimentally verified, the amount of metal iron in the green MnZn-ferrite compacts remarkably reduces the shrinkage during sintering, unfortunately however, it also reduces the final density. The decrease in the shrinkage occurs mostly because of the volume expansion due to the oxidation of the metal iron during the reaction sintering while a low final density is caused mainly by the relatively high residual porosity, which is a result of the reaction sintering.

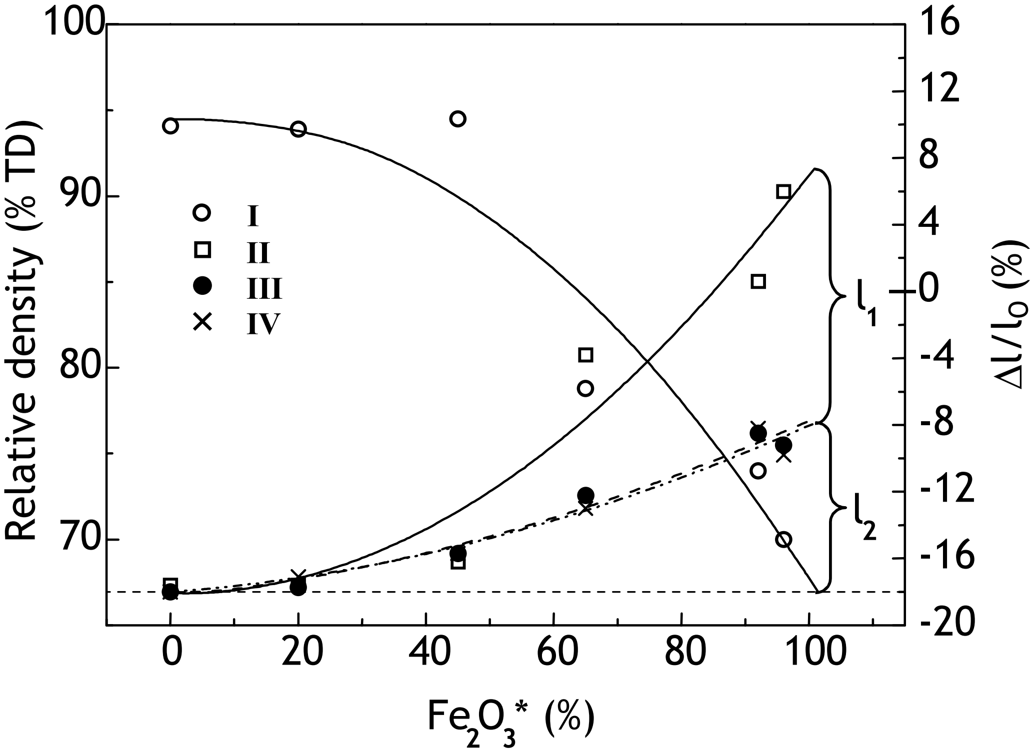

Fig. 8: The dependence of the shrinkage and density of attritor milled samples vs their compositions; 0, A, B, C, and D1 (Table I) corrected for the amount of iron oxidized during milling, Fig. 3. The increase of Fe_2O_3 in the final composition due to the erosion of the steel balls during milling was estimated to be around 0,1 wt. % per hour; (I) the density, (II) the shrinkage, (III) the shrinkage corrected for the residual porosity, (IV) dimensional change, estimated using Eq. (1), relative to the maximum shrinkage (18 %) of undoped samples with 95 % TD.

The initial shrinkage of about 18% observed during sintering of metal-iron-free samples decreases remarkably when metal iron is used. In the case, for example, when 92 % of Fe_2O_3 needed for the syntheses of MnZn ferrite was formed via metal-iron oxidation, the initial shrinkage was completely compensated, see curve II. Part of the shrinkage compensation was achieved as a result of the expansion of the samples during the oxidation of the metal iron to haematite. This part can be estimated by using the Eq.(1), see curve IV in Fig. 8. The rest of the observed total shrinkage is due to the presence of the residual porosity induced during the reaction sintering, marked as L_1 in Fig. 8. Curve III shows the total shrinkage corrected for residual porosity, $\Delta L/L = 1 - (\rho_s/ \rho_o)^{1/3}$, here ρ_s is the sintered density and ρ_o was taken as the "theoretical density", the density of the metal-iron-free samples with a shrinkage of 18%.

It can be seen that curve IV, which shows the estimated shrinkage resulting from the expansion caused by the Fe_2O_3 formed during the metal–iron oxidation in the MnZn-ferrites samples using Eq.(1), fits the curve II, showing the experimental values, i.e. shrinkage corrected for the residual porosity, reasonably well.

Fig. 8 shows that part of the shrinkage compensation has its origin in the residual porosity, which should be eliminated during sintering. When we apply intensive milling in order to decrease the residual porosity, the beneficial influence of the metal iron applied for the shrinkage-compensation during sintering is lost. An intensive attritor milling diminishes the efficiency of the metal iron added to the original mixture, due to the mechanochemical oxidation of iron. This might even destroy the starting objective, i.e. that the reaction forming caused by the metal-iron oxidation during sintering should compensate or at least strongly decrease the final shrinkage during sintering.

Thus, in order to achieve the predicted goal and to successfully control the final shrinkage by using the reaction-forming technique, a compromise must be achieved between the amount of metal iron present in the starting mixture and the milling intensity applied during the preparation of green compacts in order to optimise the microstructure and the final shrinkage.

Conclusions

- The addition of Fe to MnZn ferrite can substantially decrease the final shrinkage during sintering of MnZn ferrites in air.
- Milling of the starting raw materials increases the final density of sintered samples.
- Intensive attritor milling induces the mechanochemical oxidation of iron grains and removes the expansion ability of iron oxidation during sintering.

References

[1] A. Goldman, *Modern Ferrite Technology;* Van Nostrand Reinhold, New York, 1990.

[2] F. J. C. M. Toolenaar, M.T.J. Van Lierop-Verhees, Reactive Sintering of Manganese Ferrite, *J. Mat. Sci.* **1989**, *24*, 402-408.

[3] Y. T. Chien, Y. C. Ko, Dependance of Magnetic Properties of MnZn Ferrites on the Degree of Calcination, *J. Mat. Sci.* **1991***, 26*, 5859-64.

[4] D. Autessier, L. Autessier, *Ferrites Proc. of ICF6*, Tokyo- Kyoto, Japan, 1992, pp. 132-135.

[5] S. Wu, N. Claussen, Fabrication of Low-shrinkage Reaction-Bonded Mullite, *J. Am. Cer. Soc.***1991***, 74*, 2460-2463.

[6] S. Wu, D. Holz, N. Claussen, Mechanisms and Kinetics of Reaction-Bonded Aluminium-Bonded Oxide Ceramics, *J. Am. Cer. Soc.* **1993**, *76*, 970-980.

[7] T. Kosmač, T. M. Courtney, Milling and Mechanical Alloying of Inorganic Nonmetallics, *J. Mat. Res.* **1992**, *7*, 1519-1525.

[8] W. D. Kingery, B. Francois, *Sintering and Related Phenomena*, Ed. G. C. Kuczynski, N. A. Hooten and C. F. Sibbon, Gordon and Breach, New York, 1967, pp. 471-479.

[9] F. F. Lange, Sinterability of Agglomerated Powders, *J. Am. Cer. Soc.* **1984**, *67*, 83-89.

Povzetek

V delu poročamo o izdelavi reakcijsko vezane MnZn feritne keramike z manjšim krčenjem med sintranjem zaradi povečanja volumna, ki spremlja oksidacijo kovinskega železa.

Mlete mešanice praškov Fe_2O_3,, Mn_3O_4 in ZnO ter kovinskega železa smo stisnili v surovce in jih sintrali pri 1350 °C na zraku. Med segrevanjem se najprej oksidira železo, nastali α Fe_2O_3 pa reagira z ZnO ob tvorbi Zn ferita. Ti dve reakciji potečeta do 800 °C, v temperaturnem območju 900 °C-1300 °C pa nastaja MnZn ferit. Povečanje volumna, ki spremlja te reakcije, in razvoj poroznosti med reakcijskim sintranjem delno ali v celoti kompenzirata krčenje materiala med zgoščevanjem. Intenzivno mletje izhodnega materiala nekoliko ublaži zmanjšanje skrčka in sicer zaradi delne oksidacije kovinskega železa med mletjem in manjše poroznosti sintrane keramike.